Cross sections for charmonia dissociation in collisions with pions, rhos and kaons[*]

LIU Yan-Ju(刘延举)   XU Xiao-Ming(许晓明)[1)]   LI Yu-Qi(李玉琦)

(Department of Physics, Shanghai University, Shanghai 200444, China)

Abstract   We calculate the unpolarized cross sections for dissociation reactions of charmonia in collisions with π, ρ and K in a potential that is derived from QCD. The reactions are governed by the quark-interchange processes. The mesonic quark-antiquark relative-motion wave functions are determined by the central spin-independent terms of the potential. The numerical wave functions and cross sections are parametrized. The difference of transition amplitudes in the prior form and in the post form is explored by deriving and examining the transition amplitudes of the one-gluon-exchange spin-spin term of the potential in the two forms. We find that the post-prior discrepancy in meson-meson elastic scattering that is governed by quark-interchange processes depends on the difference of quark or antiquark masses and of quark-antiquark spatial distributions of the two mesons.

Key words   charmonium dissociation cross section, post-prior discrepancy

PACS   25.75.Nq, 25.75.-q, 12.38.Mh

1   Introduction

The observed J/ψ suppression in ultrarelativistic heavy-ion collisions comes from the dissociation of J/ψ in collisions with gluons, quarks and antiquarks in quark-gluon plasma[1, 2] as well as hadrons in hadronic matter[3]. To identify J/ψ as a probe of quark-gluon plasma[4] in a definite way the hadron-charmonium dissociation processes must be well understood. Calculations of dissociation cross sections are thus an important aspect in studying J/ψ physics. Since the dissociation processes are governed by the quark interchange mechanism, models based on the mechanism have been developed to calculate the cross sections[5—8].

In Ref. [8] the polarized cross sections for meson-charmonium reactions $q\bar{q} + c\bar{c} \rightarrow q\bar{c} + c\bar{q}$ are calculated with a potential that is derived from perturbative QCD and linear confinement. There the confinement was limited to take place only between q and $\bar{c}$ to form one charmed meson and between c and $\bar{q}$ to form another charmed meson. This is an approximation. The confinement also relates to q and c as well as $\bar{q}$ and $\bar{c}$. Since unpolarized cross sections are used in transport models of ultrarelativistic heavy-ion collisions, in the present work we present the unpolarized cross sections for π-charmonia, ρ-charmonia and K-charmonia. The pions, rhos and kaons are dominant meson species in hadronic matter produced in Au-Au collisions at the Relativistic Heavy Ion Collider energies.

A flavour rearrangement can happen in the process of the quark (antiquark) interchange between two scattering mesons. Gluon exchange is another process which determines the meson-charmonium scattering. The scattering is in the prior form shown in Fig. 1 when the gluon exchange takes place prior to the quark (antiquark) interchange and in the post form shown in Fig. 2 when the gluon exchange takes place after the quark (antiquark) interchange. Meson-charmonium scattering in the two forms may have different cross sections, which is the so-called post-prior discrepancy. We pay a particular attention to the post-prior discrepancy that results from the use of approximate quark-antiquark relative-motion wave functions[9—11]. But in elastic scattering of $\pi\pi$ and Kπ the discrepancy has been shown by numerical results to disappear[12, 13]. The cases are interesting and we therefore give analytic formulas for transition amplitudes of the reactions to explicitly exhibit the

appearance or the disappearance of the post-prior discrepancy. In the present work we use both the prior form and the post form in contrast to Ref. [8] where only the prior form was used.

In Section 2 we present formulas for cross sections and transition amplitudes. The potential and wave functions that are involved in the transition amplitudes are given. In Section 3 numerical results for cross sections, discussions and parametrizations for cross sections are shown. In Section 4 the post-prior discrepancy is investigated. In the last section is summary.
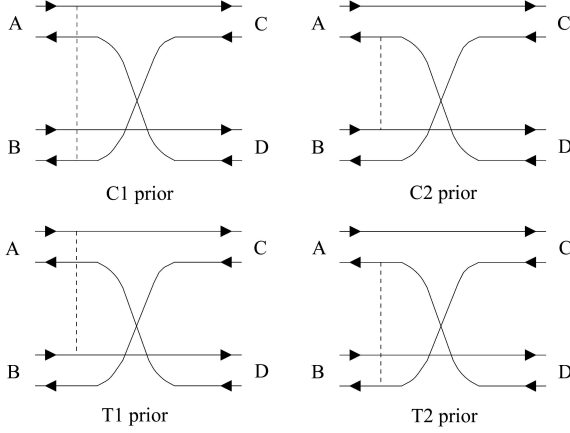

Fig. 1. "Prior" diagrams for the reaction $A + B \longrightarrow C + D$. Solid (dashed) lines represent quarks or antiquarks (gluons).
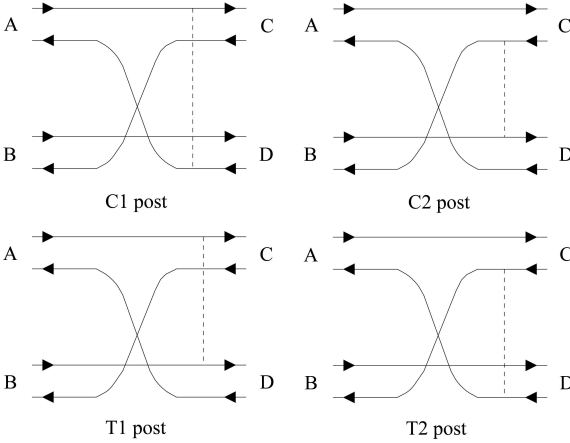

Fig. 2. The same as Fig. 1, except for "post" diagrams.

2 Formulas

We denote the energies of mesons A, B, C and D by E_A, E_B, E_C and E_D, the three-dimensional momenta by $\boldsymbol{P}_A$, $\boldsymbol{P}_B$, $\boldsymbol{P}_C$ and $\boldsymbol{P}_D$, masses by m_A, m_B, m_C and m_D, respectively. The Mandelstam variables are $s = (E_A + E_B)^2 - (\boldsymbol{P}_A + \boldsymbol{P}_B)^2$ and $t = (E_A - E_C)^2 - (\boldsymbol{P}_A - \boldsymbol{P}_C)^2$. The cross section for meson-charmonium scattering $A(q\bar{q}) + B(c\bar{c}) \to C(q\bar{c}) + D(c\bar{q})$

is[8, 14]:

$$\sigma(\sqrt{s}) = \frac{1}{32\pi s} \frac{|\boldsymbol{P}'(\sqrt{s})|}{|\boldsymbol{P}(\sqrt{s})|} \int_0^\pi d\theta |\mathcal{M}(s,t)|^2 \sin\theta , \quad (1)$$

where θ is the angle between $\boldsymbol{P}$ and $\boldsymbol{P}'$, $\boldsymbol{P}$ and $\boldsymbol{P}'$ are the three-dimensional momenta of mesons A and C in the center-of-momentum frame of the two initial mesons, respectively. $\boldsymbol{P}$ and $\boldsymbol{P}'$ are related to the Mandelstam variables s

$$|\boldsymbol{P}(\sqrt{s})|^2 = \frac{1}{4s} \left\{ [s - (m_A^2 + m_B^2)]^2 - 4m_A^2 m_B^2 \right\}, \quad (2)$$

$$|\boldsymbol{P}'(\sqrt{s})|^2 = \frac{1}{4s} \left\{ [s - (m_C^2 + m_D^2)]^2 - 4m_C^2 m_D^2 \right\}. \quad (3)$$

The transition amplitude $\mathcal{M}$ in the prior form is

$$\mathcal{M}_{\text{prior}} = 4\sqrt{E_A E_B E_C E_D} \langle \psi_{q\bar{c}} | \langle \psi_{c\bar{q}} | (V_{q\bar{c}} + V_{\bar{q}c} +$$
$$V_{qc} + V_{\bar{q}\bar{c}}) | \psi_{q\bar{q}} \rangle | \psi_{c\bar{c}} \rangle, \quad (4)$$

and in the post form is

$$\mathcal{M}_{\text{post}} = 4\sqrt{E_A E_B E_C E_D} \langle \psi_{q\bar{c}} | \langle \psi_{c\bar{q}} | (V_{q\bar{q}} + V_{\bar{c}c} +$$
$$V_{qc} + V_{\bar{q}\bar{c}}) | \psi_{q\bar{q}} \rangle | \psi_{c\bar{c}} \rangle, \quad (5)$$

where $\psi_{q\bar{q}}$, $\psi_{c\bar{c}}$, $\psi_{q\bar{c}}$ and $\psi_{c\bar{q}}$ are the wave functions of the relative motion of quark and antiquark inside the four mesons, respectively.

The unpolarized cross section

$$\sigma^{\text{unpol}}(\sqrt{s}) = \frac{1}{(2S_A + 1)(2S_B + 1)(2L_B + 1)} \times$$
$$\sum_{S L_{\text{Bz}}} (2S + 1) \sigma(S, L_{\text{Bz}}, \sqrt{s}), \quad (6)$$

where $S_A(L_A)$ and $S_B(L_B)$ are the spin quantum numbers (orbital-angular-momentum quantum numbers) of mesons A and B, respectively. $\sigma(S, L_{\text{Bz}}, \sqrt{s})$ is the polarized cross section for the reaction channel with the total spin S of the two initial mesons and the third component L_{Bz} of the orbital angular momentum of meson B, and is calculated with Eq. (1).

The potential involved in the transition amplitude is the central spin-independent potential, i.e., the Buchmüller-Tye potential[15] plus spin-spin interaction

$$V_{ab}(\boldsymbol{Q}) = \frac{\boldsymbol{\lambda}_a}{2} \cdot \frac{\boldsymbol{\lambda}_b}{2} \frac{16\pi^2 K}{\boldsymbol{Q^4}} +$$
$$\frac{\boldsymbol{\lambda}_a}{2} \cdot \frac{\boldsymbol{\lambda}_b}{2} \frac{16\pi^2}{\boldsymbol{Q^2}} \left(\rho(\boldsymbol{Q^2}) - \frac{K}{\boldsymbol{Q^2}} \right) -$$
$$\frac{\boldsymbol{\lambda}_a}{2} \cdot \frac{\boldsymbol{\lambda}_b}{2} \frac{16\pi^2}{25} \frac{\boldsymbol{s}_a \cdot \boldsymbol{s}_b}{m_a m_b} + \frac{\boldsymbol{\lambda}_a}{2} \cdot \frac{\boldsymbol{\lambda}_b}{2} \frac{16\pi^2 \lambda}{25Q} \times$$
$$\int_0^{+\infty} dx \frac{d^2 v(x)}{dx^2} \sin\left(\frac{Q}{\lambda} x \right) \frac{\boldsymbol{s}_a \cdot \boldsymbol{s}_b}{m_a m_b} , \quad (7)$$

where $\boldsymbol{Q}$ is the gluon momentum, $K = 3/16\pi^2\alpha'$ with the Regge slope $\alpha' = 1.04$ GeV^{-2}, $\lambda = \sqrt{3b_0/16\pi^2\alpha'}$ with $b_0 = 25/3$, $\boldsymbol{\lambda}_a$, $\boldsymbol{s}_a$ and m_a represent the Gell-Mann "λ-matrices", spin and mass of

constituent a, respectively. $\rho(\boldsymbol{Q}^2)$ is the running coupling constant[15] and the function $v(x)$ can be found in Ref. [15].

The quark-antiquark relative-motion wave functions involved in the transition amplitude are solutions of the Schrödinger equation with the central spin-independent potential. Assuming a charm quark mass, the Schrödinger equation was solved to get quark-antiquark relative-motion wave functions that lead to mass splittings of J/ψ, χ_{cJ} and ψ′ from the spin-spin interaction[8, 15]. While the experimental mass splittings are reproduced, a charm quark mass and numerical wave functions of J/ψ, χ_{cJ} and ψ′ are determined. The determined charm quark mass is 1.507 GeV. Similarly, the up and down (strange) quarks have mass 0.33 GeV (0.53 GeV) determined by fitting the experimental mass splitting of π and ρ (K and K*) while the numerical wave functions of π, ρ, K and K* are solutions of the Schrödinger equation[8]. With the masses of light quarks and charm quark the Schrödinger equation gives numerical wave functions

for D, D*, D_s and D_s^* that reproduce the experimental mass splittings of D and D*, D_s and D_s^* from the spin-spin interaction[8]. Fourier transform of these numerical wave functions gives their numerical representation in momentum space. Parametrizations of the numerical wave functions in momentum space are

$$\psi_{1lm}(\boldsymbol{p}) = \frac{C(pr)^l}{[(pr)^{b_1} + a_1(pr)^{b_2} + a_2(pr)^{b_3} + a_3]^{c_1}} Y_{lm} \tag{8}$$

for π, ρ, K, K*, J/ψ, χ_{cJ}, D, D*, D_s and D_s^* and

$$\psi_{2lm}(\boldsymbol{p}) = \frac{C[(pr)^{1.8} - 2.592^{1.8}]}{[(pr)^{b_1} + a_1(pr)^{b_2} + a_2(pr)^{b_3} + a_3]^{c_1}} Y_{lm} \tag{9}$$

for ψ′, p is the relative momentum of quark and antiquark, C is the normalization constant and r is meson radius. The values of a_1, a_2, a_3, b_1, b_2, b_3, c_1, r and C are listed in Table 1. The wave functions are normalized according to

$$\int \frac{\mathrm{d}^3 p}{(2\pi)^3} \psi_{nlm}^+(\boldsymbol{p}) \psi_{nlm}(\boldsymbol{p}) = 1 . \tag{10}$$

Table 1. Values of parameters in the parametrizations of wave functions.

meson	a_1	a_2	a_3	b_1	b_2	b_3	c_1	r/mf	C
J/ψ	1	1	13.7	1.2	2.4	2.8	2.1	0.412	1.25×10^3
ψ′	0.8	0	48.8	1.4	2.7		3.6	0.836	2.22×10^6
χ_{cJ}	0.9	0	37.7	1.7	2.4		4.9	0.655	1.98×10^8
π, ρ, K, K*	1	1	14	1.2	1.9	3.2	2	0.806	2.67×10^3
D, D*	1	1	12.3	1.4	1.7	3.3	1.8	0.657	9.21×10^2
D_s, D_s^*	1	1	13.5	1.4	1.9	3.1	2	0.559	1.45×10^3

3 Numerical results and discussions

We concern the following meson-charmonium reactions:

$$\pi + J/\psi \to \bar{D}^{*0}D, \bar{D}^0 D^*, \bar{D}^{*0}D^*,$$

$$\pi + \psi' \to \bar{D}^{*0}D, \bar{D}^0 D^*, \bar{D}^{*0}D^*,$$

$$\pi + \chi_{cJ} \to \bar{D}^{*0}D, \bar{D}^0 D^*, \bar{D}^{*0}D^*,$$

$$\rho + J/\psi \to \bar{D}^0 D, \bar{D}^{*0}D, \bar{D}^0 D^*, \bar{D}^{*0}D^*,$$

$$\rho + \psi' \to \bar{D}^0 D, \bar{D}^{*0}D, \bar{D}^0 D^*, \bar{D}^{*0}D^*,$$

$$\rho + \chi_{cJ} \to \bar{D}^0 D, \bar{D}^{*0}D, \bar{D}^0 D^*, \bar{D}^{*0}D^*,$$

$$K + J/\psi \to \bar{D}^{*0}D_s, \bar{D}^0 D_s^*, \bar{D}^{*0}D_s^*,$$

$$K + \psi' \to \bar{D}^{*0}D_s, \bar{D}^0 D_s^*, \bar{D}^{*0}D_s^*,$$

$$K + \chi_{cJ} \to \bar{D}^{*0}D_s, \bar{D}^0 D_s^*, \bar{D}^{*0}D_s^*.$$

Because of thermal distributions of mesons in hadronic matter, the average value of $\sqrt{s}$ of a type of meson-meson reactions in hadronic matter is not far away from the threshold energy $\sqrt{s_0}$ of the type, and

we show $\sqrt{s}$-dependence of the unpolarized meson-charmonium cross sections for π + J/ψ, π + χ_{cJ} and ρ + J/ψ in the region $\sqrt{s} < \sqrt{s_0} + 1$ GeV from Fig. 3 through Fig. 5. Due to the number of figures limited by the editorial board, the cross sections for the other reactions are not shown. The unpolarized cross section is the average of the two cross sections individually obtained in the prior form and in the post form. The threshold energy equals the total mass of the two initial mesons of an exothermic reaction or of the two final mesons of an endothermic reaction. The cross section is determined by the factors $\frac{1}{s}$, $\frac{|\boldsymbol{P}'|}{|\boldsymbol{P}|}$ and $|\mathcal{M}(s,t)|^2$. At the threshold energy $|\boldsymbol{P}'| = 0$, $|\boldsymbol{P}| \neq 0$ and $\sigma(\sqrt{s_0}) = 0$ for an endothermic reaction; $|\boldsymbol{P}'| \neq 0$, $|\boldsymbol{P}| = 0$ and $\sigma(\sqrt{s_0}) = \infty$ for an exothermic reaction. Even though the two sorts of reactions have different cross sections very near the threshold energy, they all approach zero at $\sqrt{s} \to \infty$ since $\frac{|\boldsymbol{P}'|}{|\boldsymbol{P}|}$ tends to 1 and the factors $\frac{1}{s}$ and $|\mathcal{M}(s,t)|^2$ decrease with increasing $\sqrt{s}$. The parametrizations of the quark-antiquark relative-motion wave functions address that the wave

functions decrease with the increasing relative momentum of quark and antiquark. When $\sqrt{s}$ increases, the average relative momentum of quark and antiquark in any of the incoming and outgoing mesons increases. Then the squared transition amplitude obtained from the wave functions decreases.
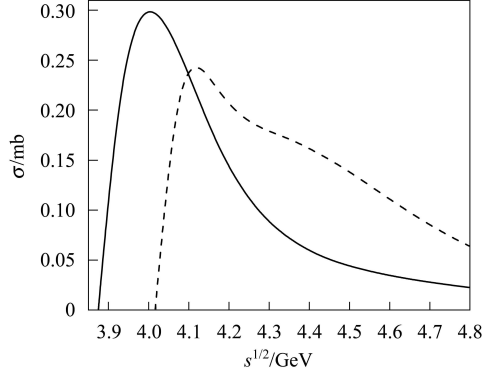

Fig. 3.　Solid and dashed curves are cross sections for $\pi + J/\psi \to \bar{D}^{*0}D$ and $\bar{D}^{*0}D^*$, respectively.
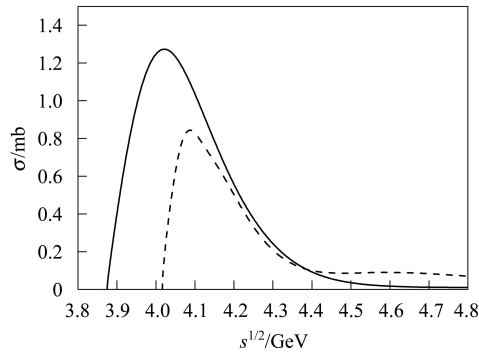

Fig. 4.　Solid and dashed curves are cross sections for $\pi + \chi_{cJ} \to \bar{D}^{*0}D$ and $\bar{D}^{*0}D^*$, respectively.
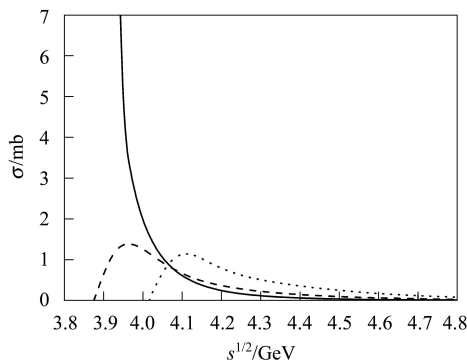

Fig. 5.　Solid, dashed and dotted curves are cross sections for $\rho + J/\psi \to \bar{D}^0D$, $\bar{D}^{*0}D$, and $\bar{D}^{*0}D^*$, respectively.

Obviously, the maxima of cross sections for $\pi + \psi'$ reactions are larger than the maxima for $\pi + \chi_{cJ}$ and the latter are larger than the ones for $\pi + J/\psi$. Similar cases maintain for the endothermic reactions of

$K + \chi_{cJ}$ and $K + J/\psi$. Increasing radius from J/ψ to χ_{cJ} and to ψ' is displayed in Table 1. A meson with a larger radius can have larger probability to react with a target meson. The difference of charmonium radii leads to the above variation of the maxima of the cross sections.

In a figure among Figs. 3—5, the two endothermic reactions have identical initial mesons. The maximum of the cross section for the reaction with two final vector mesons is smaller than the one with only one final vector meson. The difference of the maxima is controlled by $|\boldsymbol{P}'|$ which is smaller for the two final vector mesons than for only one final vector meson at the same $\sqrt{s}$.

For convenient use of the cross sections for endothermic reactions in studying J/ψ suppression we choose a simple functional form

$$\sigma(\sqrt{s}) = \sigma_{\max} \left(\frac{\epsilon}{\epsilon_{\mathrm{endo}}} \right)^a \exp \left[a \left(1 - \frac{\epsilon}{\epsilon_{\mathrm{endo}}} \right) \right], \quad (11)$$

where $\epsilon = \sqrt{s} - \sqrt{s_0}$, to fit the numerical cross sections for the endothermic reactions. The parameters a, ϵ_{endo} in unit of GeV, $\sigma_{\max}$ in unit of mb are listed in Table 2.

Table 2.　Parameters fitted to cross sections.

	$\bar{D}^{*0}D$	$\bar{D}^{*0}D^*$	$\bar{D}^{*0}D_s$	$\bar{D}^0D_s^*$	$\bar{D}^{*0}D_s^*$
$\pi J/\psi \to$					
a	0.81255	0.35511			
$\sigma_{\max}$	0.2934	0.2297			
$\epsilon_{\mathrm{endo}} - \sqrt{s_0}$	0.11638	0.12084			
$\pi\psi' \to$					
a	0.52662	0.53602			
$\sigma_{\max}$	3.61752	2.95			
$\epsilon_{\mathrm{endo}} - \sqrt{s_0}$	0.09792	0.08433			
$\pi\chi_{cJ} \to$					
a	1.6366	0.37732			
$\sigma_{\max}$	1.32991	0.93875			
$\epsilon_{\mathrm{endo}} - \sqrt{s_0}$	0.13375	0.044			
$\rho J/\psi \to$					
a	0.59269	0.42361			
$\sigma_{\max}$	1.4113	1.0998			
$\epsilon_{\mathrm{endo}} - \sqrt{s_0}$	0.0674	0.07143			
$K J/\psi \to$					
a			0.32751	0.42337	0.68168
$\sigma_{\max}$			0.27989	0.28213	0.10532
$\epsilon_{\mathrm{endo}} - \sqrt{s_0}$			0.05195	0.04856	0.2678
$K\chi_{cJ} \to$					
a					0.89602
$\sigma_{\max}$					1.86373
$\epsilon_{\mathrm{endo}} - \sqrt{s_0}$					0.07225

At present, there are no experimental data for the charmonia dissociation cross sections in both free space and hadronic matter at finite temperature and density. However, the present method for studying

the charmonia dissociation can be extended to calculate the cross sections with medium effect. At finite temperature the confinement gets weak and the linear confinement should be replaced by plateau form obtained in lattice gauge calculations[16]. With such a potential modified by medium quark-antiquark relative-motion wave functions have larger spatial extension than those related to the linear confinement in free space. Then the charmonia dissociation cross sections are expected to become larger in hadronic matter.

4 The prior form and the post form

At the first sight of the transition amplitudes in the prior form and in the post form, the difference between the first two terms in Eq. (4) and the ones in Eq. (5) makes $\mathcal{M}_{\mathrm{prior}} \neq \mathcal{M}_{\mathrm{post}}$ possible. However, as long as the quark-antiquark wave functions are eigenfunctions of the potential (7), $\mathcal{M}_{\mathrm{prior}} = \mathcal{M}_{\mathrm{post}}$ is ensured according to the proofs in Refs. [9] and [10]. If the quark-antiquark wave functions are not eigenfunctions of the potential, i.e., are approximate wave functions to the eigenfunctions, $\mathcal{M}_{\mathrm{prior}}$ will not equal $\mathcal{M}_{\mathrm{post}}$ as shown by the discrepancy of the cross sections in the prior form and in the post form in Fig. 6. The approximate wave functions in the present work are given by the Schrödinger equation with the central spin-independent terms of the potential. Nevertheless, there is no post-prior discrepancy in the elastic scattering of the $I = 2$ $\pi\pi$[12, 13] and the $I = 3/2$ $\mathrm{K}\pi$[13]. This is observed from the numerical calculations of S-wave phase shifts, but the reason is not clear. In this section we derive analytic expressions of the transition amplitudes in the prior from and in the post form with the tree-level spin-spin term $-\dfrac{\boldsymbol{\lambda}_a}{2} \cdot \dfrac{\boldsymbol{\lambda}_b}{2} \dfrac{16\pi^2}{25} \dfrac{\boldsymbol{s}_a \cdot \boldsymbol{s}_b}{m_a m_b}$ to find the reason for the equivalence of $\mathcal{M}_{\mathrm{prior}}$ and $\mathcal{M}_{\mathrm{post}}$.
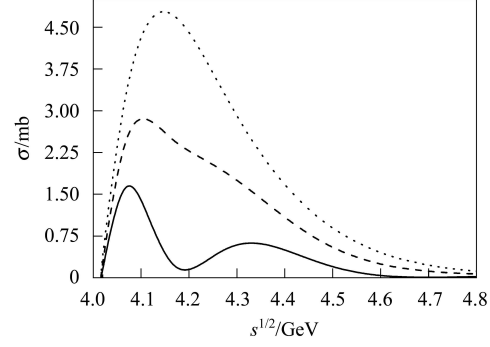
Fig. 6. Cross sections for $\pi + \psi' \rightarrow \bar{\mathrm{D}}^{*0} + \mathrm{D}^*$. Solid curve: the post form; dashed curve: the average value; dotted curve: the prior form.

The quark-antiquark relative-motion wave functions in momentum space can also be parametrized as

$$\psi_{\mathrm{q\bar{q}}} = (8\pi\alpha_1)^{3/4} \mathrm{e}^{-\alpha_1 \boldsymbol{p}_{\mathrm{q\bar{q}}}^2}, \qquad \psi_{\mathrm{c\bar{c}}} = (8\pi\alpha_2)^{3/4} \mathrm{e}^{-\alpha_2 \boldsymbol{p}_{\mathrm{c\bar{c}}}^2},$$

for the initial mesons and

$$\psi_{\mathrm{q\bar{c}}} = (8\pi\alpha_3)^{3/4} \mathrm{e}^{-\alpha_3 \boldsymbol{p}_{\mathrm{q\bar{c}}}^2}, \qquad \psi_{\mathrm{c\bar{q}}} = (8\pi\alpha_4)^{3/4} \mathrm{e}^{-\alpha_4 \boldsymbol{p}_{\mathrm{c\bar{q}}}^2},$$

for the final mesons. $\boldsymbol{p}_{ab}$ means relative momentum of constituents a and b. α_1, α_2, α_3 and α_4 are constants. The four wave functions satisfy the normalization condition (10). Fitted to Fourier transform of the numerical solutions of the Schrödinger equation with the central spin-independent potential, the parameters α_1, α_2, α_3 and α_4 take values 0.0621 fm² for J/ψ, 0.2284 fm² for π, ρ, K and K*, 0.1599 fm² for D and D*, 0.1168 fm² for $\mathrm{D_s}$ and $\mathrm{D_s^*}$.

The matrix element of the spin-spin term is

$$I = -\langle\psi_{\mathrm{q\bar{c}}}|\langle\psi_{\mathrm{c\bar{q}}}| \frac{\boldsymbol{\lambda}_a}{2} \cdot \frac{\boldsymbol{\lambda}_b}{2} \frac{16\pi^2}{25} \frac{\boldsymbol{s}_a \cdot \boldsymbol{s}_b}{m_a m_b} |\psi_{\mathrm{q\bar{q}}}\rangle|\psi_{\mathrm{c\bar{c}}}\rangle.$$

For the quark-interchange processes in the prior form and in the post form the matrix element is

$$I^{\mathrm{C1prior}} = -\frac{128\pi^2}{25} \frac{\boldsymbol{\lambda}_{\mathrm{q}}}{2} \cdot \frac{\boldsymbol{\lambda}_{\bar{\mathrm{c}}}}{2} \frac{\boldsymbol{s}_{\mathrm{q}} \cdot \boldsymbol{s}_{\bar{\mathrm{c}}}}{m_{\mathrm{q}} m_{\bar{\mathrm{c}}}} \frac{(\alpha_1\alpha_2\alpha_3\alpha_4)^{3/4}}{[(\alpha_1+\alpha_2+\alpha_4)\alpha_3]^{3/2}} \exp\Bigg\{ -\Bigg[\left(\frac{m_{\mathrm{q}}}{m_{\mathrm{q}}+m_{\bar{\mathrm{q}}}}\boldsymbol{P}\right)^2 \alpha_1 + \left(\frac{m_{\bar{\mathrm{c}}}}{m_{\mathrm{c}}+m_{\bar{\mathrm{c}}}}\boldsymbol{P}+\boldsymbol{P}'\right)^2 \alpha_2 +$$
$$\left(\boldsymbol{P}+\frac{m_{\bar{\mathrm{q}}}}{m_{\mathrm{c}}+m_{\bar{\mathrm{q}}}}\boldsymbol{P}'\right)^2 \alpha_4 \Bigg] + \frac{\left[\left(\frac{m_{\mathrm{q}}}{m_{\mathrm{q}}+m_{\bar{\mathrm{q}}}}\boldsymbol{P}\right)\alpha_1 + \left(\frac{m_{\bar{\mathrm{c}}}}{m_{\mathrm{c}}+m_{\bar{\mathrm{c}}}}\boldsymbol{P}+\boldsymbol{P}'\right)\alpha_2 + \left(\boldsymbol{P}+\frac{m_{\bar{\mathrm{q}}}}{m_{\mathrm{c}}+m_{\bar{\mathrm{q}}}}\boldsymbol{P}'\right)\alpha_4 \right]^2}{\alpha_1+\alpha_2+\alpha_4} \Bigg\}, \quad (12)$$

$$I^{\mathrm{C2prior}} = -\frac{128\pi^2}{25} \frac{\boldsymbol{\lambda}_{\bar{\mathrm{q}}}}{2} \cdot \frac{\boldsymbol{\lambda}_{\mathrm{c}}}{2} \frac{\boldsymbol{s}_{\bar{\mathrm{q}}} \cdot \boldsymbol{s}_{\mathrm{c}}}{m_{\bar{\mathrm{q}}} m_{\mathrm{c}}} \frac{(\alpha_1\alpha_2\alpha_3\alpha_4)^{3/4}}{[(\alpha_1+\alpha_2+\alpha_3)\alpha_4]^{3/2}} \exp\Bigg\{ -\Bigg[\left(\frac{m_{\bar{\mathrm{q}}}}{m_{\mathrm{q}}+m_{\bar{\mathrm{q}}}}\boldsymbol{P}\right)^2 \alpha_1 + \left(\frac{m_{\mathrm{c}}}{m_{\mathrm{c}}+m_{\bar{\mathrm{c}}}}\boldsymbol{P}-\boldsymbol{P}'\right)^2 \alpha_2 +$$
$$\left(\boldsymbol{P}-\frac{m_{\mathrm{q}}}{m_{\mathrm{q}}+m_{\bar{\mathrm{c}}}}\boldsymbol{P}'\right)^2 \alpha_3 \Bigg] + \frac{\left[\left(\frac{m_{\bar{\mathrm{q}}}}{m_{\mathrm{q}}+m_{\bar{\mathrm{q}}}}\boldsymbol{P}\right)\alpha_1 + \left(\frac{m_{\mathrm{c}}}{m_{\mathrm{c}}+m_{\bar{\mathrm{c}}}}\boldsymbol{P}-\boldsymbol{P}'\right)\alpha_2 + \left(\boldsymbol{P}-\frac{m_{\mathrm{q}}}{m_{\mathrm{q}}+m_{\bar{\mathrm{c}}}}\boldsymbol{P}'\right)\alpha_3 \right]^2}{\alpha_1+\alpha_2+\alpha_3} \Bigg\}, \quad (13)$$

$$I^{\mathrm{T1prior}} = -\frac{128\pi^2}{25}\frac{\boldsymbol{\lambda}_q}{2}\cdot\frac{\boldsymbol{\lambda}_c}{2}\frac{\boldsymbol{s}_q\cdot\boldsymbol{s}_c}{m_q m_c}\frac{(\alpha_1\alpha_2\alpha_3\alpha_4)^{3/4}}{[(\alpha_1+\alpha_4)(\alpha_2+\alpha_3)]^{3/2}}\exp\Bigg\{-\Bigg[\left(\frac{m_q}{m_q+m_{\bar{q}}}\boldsymbol{P}\right)^2\alpha_1+\left(\frac{m_{\bar{c}}}{m_c+m_{\bar{c}}}\boldsymbol{P}+\boldsymbol{P}'\right)^2\alpha_2+$$

$$\left(\frac{m_q}{m_q+m_{\bar{c}}}\boldsymbol{P}'\right)^2\alpha_3+\left(\boldsymbol{P}+\frac{m_{\bar{q}}}{m_c+m_{\bar{q}}}\boldsymbol{P}'\right)^2\alpha_4\Bigg]+\frac{\left[\left(\frac{m_q}{m_q+m_{\bar{q}}}\boldsymbol{P}\right)\alpha_1+\left(\boldsymbol{P}+\frac{m_{\bar{q}}}{m_c+m_{\bar{q}}}\boldsymbol{P}'\right)\alpha_4\right]^2}{\alpha_1+\alpha_4}+$$

$$\frac{\left[\left(\frac{m_{\bar{c}}}{m_c+m_{\bar{c}}}\boldsymbol{P}+\boldsymbol{P}'\right)\alpha_2+\left(\frac{m_q}{m_q+m_{\bar{c}}}\boldsymbol{P}'\right)\alpha_3\right]^2}{\alpha_2+\alpha_3}\Bigg\}, \tag{14}$$

$$I^{\mathrm{T2prior}} = -\frac{128\pi^2}{25}\frac{\boldsymbol{\lambda}_{\bar{q}}}{2}\cdot\frac{\boldsymbol{\lambda}_{\bar{c}}}{2}\frac{\boldsymbol{s}_{\bar{q}}\cdot\boldsymbol{s}_{\bar{c}}}{m_{\bar{q}} m_{\bar{c}}}\frac{(\alpha_1\alpha_2\alpha_3\alpha_4)^{3/4}}{[(\alpha_1+\alpha_3)(\alpha_2+\alpha_4)]^{3/2}}\exp\Bigg\{-\Bigg[\left(\frac{m_{\bar{q}}}{m_q+m_{\bar{q}}}\boldsymbol{P}\right)^2\alpha_1+\left(\frac{m_c}{m_c+m_{\bar{c}}}\boldsymbol{P}-\boldsymbol{P}'\right)^2\alpha_2+$$

$$\left(\boldsymbol{P}-\frac{m_q}{m_q+m_{\bar{c}}}\boldsymbol{P}'\right)^2\alpha_3+\left(\frac{m_{\bar{q}}}{m_c+m_{\bar{q}}}\boldsymbol{P}'\right)^2\alpha_4\Bigg]+\frac{\left[\left(\frac{m_{\bar{q}}}{m_q+m_{\bar{q}}}\boldsymbol{P}\right)\alpha_1+\left(\boldsymbol{P}-\frac{m_q}{m_q+m_{\bar{c}}}\boldsymbol{P}'\right)\alpha_3\right]^2}{\alpha_1+\alpha_3}+$$

$$\frac{\left[\left(\frac{m_c}{m_c+m_{\bar{c}}}\boldsymbol{P}-\boldsymbol{P}'\right)\alpha_2+\left(\frac{m_{\bar{q}}}{m_c+m_{\bar{q}}}\boldsymbol{P}'\right)\alpha_4\right]^2}{\alpha_2+\alpha_4}\Bigg\}, \tag{15}$$

$$I^{\mathrm{C1post}} = -\frac{128\pi^2}{25}\frac{\boldsymbol{\lambda}_q}{2}\cdot\frac{\boldsymbol{\lambda}_{\bar{q}}}{2}\frac{\boldsymbol{s}_q\cdot\boldsymbol{s}_{\bar{q}}}{m_q m_{\bar{q}}}\frac{(\alpha_1\alpha_2\alpha_3\alpha_4)^{3/4}}{[\alpha_1(\alpha_2+\alpha_3+\alpha_4)]^{3/2}}\exp\Bigg\{-\Bigg[\left(\frac{m_{\bar{c}}}{m_c+m_{\bar{c}}}\boldsymbol{P}+\boldsymbol{P}'\right)^2\alpha_2+\left(\frac{m_q}{m_q+m_{\bar{c}}}\boldsymbol{P}'\right)^2\alpha_3+$$

$$\left(\boldsymbol{P}+\frac{m_{\bar{q}}}{m_c+m_{\bar{q}}}\boldsymbol{P}'\right)^2\alpha_4\Bigg]+\frac{\left[\left(\frac{m_{\bar{c}}}{m_c+m_{\bar{c}}}\boldsymbol{P}+\boldsymbol{P}'\right)\alpha_2+\left(\frac{m_q}{m_q+m_{\bar{c}}}\boldsymbol{P}'\right)\alpha_3+\left(\boldsymbol{P}+\frac{m_{\bar{q}}}{m_c+m_{\bar{q}}}\boldsymbol{P}'\right)\alpha_4\right]^2}{\alpha_2+\alpha_3+\alpha_4}\Bigg\}, \tag{16}$$

$$I^{\mathrm{C2post}} = -\frac{128\pi^2}{25}\frac{\boldsymbol{\lambda}_c}{2}\cdot\frac{\boldsymbol{\lambda}_{\bar{c}}}{2}\frac{\boldsymbol{s}_c\cdot\boldsymbol{s}_{\bar{c}}}{m_c m_{\bar{c}}}\frac{(\alpha_1\alpha_2\alpha_3\alpha_4)^{3/4}}{[(\alpha_1+\alpha_3+\alpha_4)\alpha_2]^{3/2}}\exp\Bigg\{-\Bigg[\left(\frac{m_q}{m_q+m_{\bar{q}}}\boldsymbol{P}-\boldsymbol{P}'\right)^2\alpha_1+\left(\frac{m_{\bar{c}}}{m_q+m_{\bar{c}}}\boldsymbol{P}'\right)^2\alpha_3+$$

$$\left(\boldsymbol{P}-\frac{m_c}{m_c+m_{\bar{q}}}\boldsymbol{P}'\right)^2\alpha_4\Bigg]+\frac{\left[\left(\frac{m_q}{m_q+m_{\bar{q}}}\boldsymbol{P}-\boldsymbol{P}'\right)\alpha_1-\left(\frac{m_{\bar{c}}}{m_q+m_{\bar{c}}}\boldsymbol{P}'\right)\alpha_3+\left(\boldsymbol{P}-\frac{m_c}{m_c+m_{\bar{q}}}\boldsymbol{P}'\right)\alpha_4\right]^2}{\alpha_1+\alpha_3+\alpha_4}\Bigg\}, \tag{17}$$

$$I^{\mathrm{T1post}} = I^{\mathrm{T1prior}}, \tag{18}$$

$$I^{\mathrm{T2post}} = I^{\mathrm{T2prior}}. \tag{19}$$

For the concerned meson-J/ψ reactions $m_q \neq m_c$, $m_{\bar{q}} \neq m_{\bar{c}}$ and $\alpha_1 \neq \alpha_2$. No one of I^{C1prior} and I^{C2prior} equals one of I^{C1post} and I^{C2post}. Therefore, the post-prior discrepancy happens in the meson-J/ψ dissociation reactions.

Regarding the elastic scattering of $\pi\pi$ and Kπ, $m_q = m_c$, $|\boldsymbol{P}| = |\boldsymbol{P}'|$ and the quark-antiquark relative-motion wave functions of π and K in momentum space are taken to be the same, i.e., $\alpha_1 = \alpha_2 = \alpha_3 = \alpha_4 = \alpha$. Then the matrix elements I^{C1prior}, I^{C2prior}, I^{C1post} and I^{C2post} are simplified to

$$I^{\mathrm{C1prior}} = -\frac{128\pi^2}{75\sqrt{3}m_q m_{\bar{c}}}\left(-\frac{4}{9}\right)\left(-\frac{3}{8}\right)\times$$
$$\exp\Bigg\{\frac{2}{3}[-2+2R_{\bar{q}}+2R_{\bar{c}}-2R_{\bar{q}}^2-R_{\bar{c}}^2-$$
$$R_{\bar{q}}R_{\bar{c}}+(2-2R_{\bar{q}}-2R_{\bar{c}}-R_{\bar{q}}^2+$$
$$R_{\bar{q}}R_{\bar{c}})\cos\theta]\boldsymbol{P}^2\alpha\Bigg\}, \tag{20}$$

$$I^{\mathrm{C2prior}} = -\frac{128\pi^2}{75\sqrt{3}m_q m_{\bar{q}}}\left(-\frac{4}{9}\right)\left(-\frac{3}{8}\right)\times$$
$$\exp\Bigg\{\frac{2}{3}[-2+2R_{\bar{q}}+2R_{\bar{c}}-R_{\bar{q}}^2-2R_{\bar{c}}^2-$$
$$R_{\bar{q}}R_{\bar{c}}+(2-2R_{\bar{q}}-2R_{\bar{c}}-R_{\bar{c}}^2+$$
$$R_{\bar{q}}R_{\bar{c}})\cos\theta]\boldsymbol{P}^2\alpha\Bigg\}, \tag{21}$$

$$I^{\mathrm{C1post}} = -\frac{128\pi^2}{75\sqrt{3}m_q m_{\bar{q}}}\left(-\frac{4}{9}\right)\left(-\frac{3}{8}\right)\times$$
$$\exp\Bigg\{\frac{2}{3}[-2+2R_{\bar{q}}+2R_{\bar{c}}-R_{\bar{q}}^2-2R_{\bar{c}}^2-$$
$$R_{\bar{q}}R_{\bar{c}}+(2-2R_{\bar{q}}-2R_{\bar{c}}-R_{\bar{c}}^2+$$
$$R_{\bar{q}}R_{\bar{c}})\cos\theta]\boldsymbol{P}^2\alpha\Bigg\}, \tag{22}$$

$$I^{\mathrm{C2post}} = -\frac{128\pi^2}{75\sqrt{3}m_q m_{\bar{c}}}\left(-\frac{4}{9}\right)\left(-\frac{3}{8}\right)\times$$
$$\exp\Bigg\{\frac{2}{3}[-2+2R_{\bar{q}}+2R_{\bar{c}}-2R_{\bar{q}}^2-$$
$$R_{\bar{c}}^2-R_{\bar{q}}R_{\bar{c}}+(2-2R_{\bar{q}}-2R_{\bar{c}}-R_{\bar{q}}^2+$$
$$R_{\bar{q}}R_{\bar{c}})\cos\theta]\boldsymbol{P}^2\alpha\Bigg\}. \tag{23}$$

with $R_{\bar{q}} = \dfrac{m_{\bar{q}}}{m_q + m_{\bar{q}}}$ and $R_{\bar{c}} = \dfrac{m_{\bar{c}}}{m_q + m_{\bar{c}}}$.

Apparently,

$$I^{\mathrm{C1prior}} = I^{\mathrm{C2post}}, \qquad I^{\mathrm{C2prior}} = I^{\mathrm{C1post}}. \qquad (24)$$

If $m_{\bar{q}} = m_{\bar{c}}$, $I^{\mathrm{C1prior}} = I^{\mathrm{C2prior}} = I^{\mathrm{C1post}} = I^{\mathrm{C2post}}$. The transition amplitudes with the one-gluon-exchange spin-spin term are

$$\mathcal{M}_{\mathrm{prior}}^{\mathrm{ss}} = 4\sqrt{E_A E_B E_C E_D}(I^{\mathrm{C1prior}} +$$
$$I^{\mathrm{C2prior}} + I^{\mathrm{T1prior}} + I^{\mathrm{T2prior}}), \qquad (25)$$

$$\mathcal{M}_{\mathrm{post}}^{\mathrm{ss}} = 4\sqrt{E_A E_B E_C E_D}(I^{\mathrm{C1post}} +$$
$$I^{\mathrm{C2post}} + I^{\mathrm{T1post}} + I^{\mathrm{T2post}}), \qquad (26)$$

which possess the relation

$$\mathcal{M}_{\mathrm{prior}}^{\mathrm{ss}} = \mathcal{M}_{\mathrm{post}}^{\mathrm{ss}}, \qquad (27)$$

as long as $m_q = m_c$ and whether $m_{\bar{q}} = m_{\bar{c}}$ or not. This relation is obtained without the specification of α. Since all the mesons in the ground-state pseudoscalar octet and the ground-state vector nonet can be assumed to have the same spatial wave function of the quark-antiquark relative motion[8, 13], the relation holds for elastic scattering of any two mesons in the octet and the nonet if the quarks or the antiquarks of the two mesons are of the same flavor. About elastic meson-meson scattering that is governed by the quark-interchange processes, the impossible cases are: $m_q = m_{\bar{c}}$ and $m_c \neq m_{\bar{q}}$; $m_c = m_{\bar{q}}$ and $m_q \neq m_{\bar{c}}$; $m_q = m_{\bar{c}}$ and $m_c = m_{\bar{q}}$.

Simple analytic expressions of the transition amplitudes with the terms except the third term on the right-hand side of Eq. (7) can not be obtained since the involved integrands are complicated. However, numerical calculations show that the transition amplitude with the central spin-independent terms and the loop-level spin-spin term in the prior form equals the one in the post form.

The results of the above reasoning are that the transition amplitude of the potential (7) in the prior form equals the one in the post form and there is no post-prior discrepancy of S-wave elastic phase shifts for $I = 2$ $\pi\pi$ and $I = 3/2$ Kπ scattering. The reason for the disappearance of the post-prior discrepancy is that the quarks or the antiquarks of the two mesons in elastic scattering have the same flavor and the wave functions of the quark-antiquark relative motion of mesons A, B, C and D in momentum space are identical.

5   Summary

We have obtained the unpolarized cross sections for π-charmonium, ρ-charmonium and K-charmonium dissociation reactions that are governed by the quark-interchange processes. The transition amplitudes are calculated with the potential from QCD and quark-antiquark wave functions that are given by the central spin-independent terms of the potential. The cross sections depend on the center-of-mass energy $\sqrt{s}$, the masses and spins of the initial and final mesons. The cross sections for endothermic reactions are parametrized for convenient applications. Cross sections for the production of $\bar{D}^0 D^*$ equal those of $\bar{D}^{*0} D$ and similar equalities almost hold for $\bar{D}^0 D_s^*$ and $\bar{D}^{*0} D_s$.

The post-prior discrepancy exists in meson-meson inelastic sacttering like charmonium dissociation in collisions with π, ρ and K when the approximate wave functions of quark-antiquark relative motion in mesons are used. However, in elastic scattering of the $I = 2$ $\pi\pi$ and the $I = 3/2$ Kπ the post-prior discrepancy disappears while the wave functions of quark-antiquark relative motion inside π and K take the same approximate wave function. This is clearly shown by the simple analytic expressions of the transition amplitudes corresponding to the tree-level spin-spin interaction in the prior form and in the post form. The discrepancy in meson-meson elastic scattering that is governed by the quark-interchange processes depends on the difference of quark or antiquark masses and of quark-antiquark spatial distributions of the two mesons.

References

1   Peskin M E. Nucl. Phys. B, 1979, **156**: 365; Bhanot G, Peskin M E. Nucl. Phys. B, 1979, **156**: 391
2   Kharzeev D, Satz H. Phys. Lett. B, 1994, **334**: 155
3   Ftáčnik J, Lichard P, Pišút J. Phys. Lett. B, 1988, **207**: 194; Gavin S, Gyulassy M, Jackson A. Phys. Lett. B, 1988, **207**: 257; Vogt R, Prakash M, Koch P, Hansson T H. Phys. Lett. B, 1988, **207**: 263; Gerschel C, Hüfner J. Phys. Lett. B, 1988, **207**: 253
4   Matsui T, Satz H. Phys. Lett. B, 1986, **178**: 416
5   Martins K, Blaschke D, Quack E. Phys. Rev. C, 1995, **51**: 2723
6   Wong C Y, Swanson E S, Barnes T. Phys. Rev. C, 2001, **65**: 014903
7   Barnes T, Swanson E S, Wong C Y, XU X M. Phys. Rev. C, 2003, **68**: 014903

8   XU X M. Nucl. Phys. A, 2002, **697**: 825
9   Schiff L I. Quantum Mechanics. New York: McGraw-Hill, 1968
10   Wong C Y, Crater H W. Phys. Rev. C, 2001, **63**: 044907
11   Barnes T, Black N, Swanson E S. Phys. Rev. C, 2001, **63**: 025204
12   Barnes T, Swanson E S. Phys. Rev. D, 1992, **46**: 131; Swanson E S. Ann. Phys., 1992, **220**: 73
13   LI Y Q, XU X M. Nucl. Phys. A, 2007, **794**: 210
14   XU X M, SHEN W Q, FENG Y C, ZHOU D C. Nucl. Phys. A, 2003, **713**: 470
15   Buchmüller W, Tye S H H. Phys. Rev. D, 1981, **24**: 132
16   Karsch F, Laermann E, Peikert A. Nucl. Phys. B, 2001, **605**: 579